Light transmission through a single cylindrical hole in a metallic film

F. J. García de Abajo

Centro Mixto CSIC-UPV/EHU and Donostia International Physics Center (DIPC), Aptdo. 1072, 20080 San Sebastián, Spain

jga@sw.ehu.es

http://dipc.ehu.es/jga

Abstract: The transmission of light through a subwavelength hole drilled in a metallic thin film is calculated by numerically solving Maxwell's equations both for a simple hole and for a hole with additional structure. A maximum in the transmission cross section is observed for hole diameters of the order of but smaller than the wavelength. Transmission cross sections well above the hole area are shown to be attainable by filling the hole with a high-index material. The effect of adding a small particle inside the hole is also analyzed.

OCIS codes: (050.1220) Apertures; (050.1960) Diffraction theory

References and links

1. T. W. Ebbesen, H. J. Lezec, H. F. Ghaemi, T. Thio, and P. A. Wolff, "Extraordinary optical transmission through subwavelength hole arrays," Nature **391**, 667 (1998).
2. T. Thio, K. M. Pellerin, R. A. Linke, H. J. Lezec, , and T. W. Ebbesen, "Enhanced light transmission through a single subwavelength aperture," Optics Letters **26**, 1972 (2001).
3. H. J. Lezec, A. Degiron, E. Devaux, R. A. Linke, L. Martín-Moreno, F. J. García-Vidal, and T. W. Ebbesen, "Beaming light from a subwavelength aperture," Science **297**, 820 (2002).
4. U. Schröter and D. Heitmann, "Surface-plamon-enhanced transmission through metallic gratings," Phys. Rev. B **58**, 15419 (1998).
5. Y. Takakura, "Optical resonance in a narrow slit in a thick metallic screen," Phys. Rev. Lett. **86**, 5601 (2001).
6. F. Yang and J. R. Sambles, "Resonant transmission of microwaves through a narrow metallic slit," Phys. Rev. Lett. **89**, 63901 (2002).
7. H. A. Bethe, "Theory of diffraction by small holes," Phys. Rev. **66**, 163 (1944).
8. C. J. Bouwkamp, "Diffraction theory," Reports on Progress in Physics **XVIII**, 35 (1954).
9. R. Wannemacher, "Plasmon-supported transmission of light through nanometric holes in metallic thin films," Opt. Comm. **195**, 107 (2001).
10. F. J. García de Abajo and A. Howie, "Relativistic electron energy loss and electron induced photon emission in inhomogeneous dielectrics," Phys. Rev. Lett. **80**, 5180 (1998); "Retarded field calculation of electron energy loss in inhomogeneous dielectrics", Phys. Rev. B **65**, 115418 (2002).
11. J. Aizpurua, P. Hanarp, D. S. Sutherland, M. Käll, G. W. Bryant, and F. J. García de Abajo, "Optical properties of gold nanorings," submitted to Phys. Rev. Lett.
12. When Maxwell's equations are satisfied at both sides of a given interface, the continuity of the parallel components of the electric field and the magnetic field implies the continuity of the normal electric displacement and the normal magnetic induction.
13. J. A. Porto, F. J. García-Vidal, and J. B. Pendry, "Transmission resonances on metallic gratings with very narrow slits," Phys. Rev. Lett. **83**, 2845 (1999).
14. S. Astilean, Ph. Lalanne, and M. Palamaru, "Light transmission through metallic channels much smaller than the wavelength," Opt. Comm. **175**, 265 (2000).
15. Q. Cao and Ph. Lalanne, "Negative role of surface plasmons in the transmission of metallic gratings with very narrow slits," Phys. Rev. Lett. **88**, 057403 (2002).

#1768 - $15.00 US
Received October 28, 2002; Revised December 03, 2002

The limit imposed by diffraction on the wavelength scale has been recently challenged by new photonic designs aimed at transmitting light through subwavelength apertures. In this context, extraordinary light transmission through arrays of holes has been reported [1]. Also, the transmission through isolated apertures in metallic films has been shown to be enhanced when the entrance surface is decorated with appropriate additional structure [2] and the angular distribution of the transmitted light is focused around the direction of the incoming beam when the exit surface is also decorated [3]. For narrow slits and light polarization perpendicular to the aperture, the transmission has also been shown to reach values that are several orders of magnitude higher than those expected from the geometrical area of the aperture in the absence of diffraction effects [4, 5, 6].

For circular holes in thin metallic films, light transmission becomes very small when the wavelength λ is much larger than the radius of the hole a. Actually, the transmission behaves like $\propto (a/\lambda)^4$ in the long wavelength limit, a result first obtained by Bethe [7], and subsequently corrected to include higher-order terms by Bouwkamp [8]. However, the behavior in the $\lambda \sim a$ region cannot be easily addressed by analytical means and numerical simulation becomes essential.

The infinite extension of the film becomes difficult to handle by numerical methods. In particular, finite-difference in the time domain calculations require a finite integration area of diameter R, and the numerical results show a poor convergence with R for transmission through a hole, which reflects the fact that the currents and charges induced near the hole produce a field of strength proportional to $1/R$ near the film boundary, and this acts back on the hole region with an overall strength also proportional to $1/R$ (notice that a factor of $2\pi R$ for the film circumference needs to be invoked in this argument). Therefore, it is convenient to use a method that can project the entire problem onto the region near the hole. One possibility is to use mode-expansion matching techniques [9], which are difficult to adapt to geometries as those discussed in the final part of this paper. Instead, projection on the hole region can be accomplished by using the more versatile boundary element method, as explained below.

In what follows, the boundary element method will be used to solve Maxwell's equations numerically in the presence of a perfect-metal film. This method consists in expressing the electromagnetic field in terms of boundary charges and currents within each homogeneous region of the geometry under consideration. The boundary sources are in turn obtained by imposing the customary boundary conditions on the electromagnetic field. This method has already been applied to other problems like the simulation of electron low-energy losses in the presence of complex targets [10] and also to calculate extinction cross sections of nanoparticles [11]. A modified version of this method will be discussed next that is more suitable to deal with the specific geometry of the hole under consideration.

The electromagnetic field inside a region j filled with a homogeneous material described by its dielectric function ϵ_j and magnetic permeability μ_j can be expressed in terms of equivalent electric currents and charges (σ_j and $\mathbf{h}_j$, respectively) distributed on its boundary. These sources describe the outer electromagnetic environment as observed from region j. Working in frequency space ω and using the continuity equation (i.e., $\nabla \cdot \mathbf{h}_j = \mathrm{i}\omega\sigma_j$), the electric and magnetic fields inside j can be written

$$\mathbf{E}(\mathbf{r}) = \mathbf{E}_j^{\mathrm{ext}} + \mathrm{i}k \int_{S_j} d\mathbf{s}\, [1 + \frac{1}{k^2 \epsilon_j \mu_j} \nabla\nabla] G_j(\mathbf{r} - \mathbf{s}) \mathbf{h}_j(\mathbf{s})$$

#1768 - $15.00 US Received October 28, 2002; Revised December 03, 2002

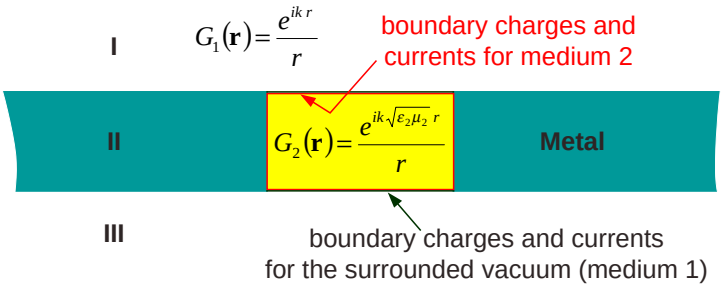

Fig. 1. Boundary element method approach to the transmission through a small hole. The problem is solved in terms of magnetic boundary charges and currents distributed around the hole boundary. See text for more details.

and

$$\mathbf{H}(\mathbf{r}) = \mathbf{H}_j^{\text{ext}} + \frac{1}{\mu_j}\int_{S_j} d\mathbf{s}\,\nabla G_j(\mathbf{r}-\mathbf{s}) \times \mathbf{h}_j(\mathbf{s}),$$

where $k = \omega/c$ is the momentum of light in vacuum, S_j represents the boundary of region j, and $\mathbf{E}_j^{\text{ext}}$ and $\mathbf{H}_j^{\text{ext}}$ are external fields with sources inside j. One can recognize the presence of the Greenean of Maxwell's equations $[1 + (1/k^2\epsilon_j\mu_j)\nabla\nabla]G_j$ in the first of these expressions, whereas the second one is directly obtained from the first using Fadaray's law. The scalar Green function $G_j(r) = \exp(\mathrm{i}k\sqrt{\epsilon_j\mu_j}r)/r$ has also been employed. Now, it is well known that, in the absence of external sources, Maxwell's equations are invariant under the transformation $\{\epsilon \to \mu, \mu \to \epsilon, \mathbf{E} \to \mathbf{H}, \mathbf{H} \to -\mathbf{E}\}$, and therefore, one might as well use magnetic boundary charges and currents instead of electric ones, so that an entirely equivalent formulation of the boundary element method can be given based upon the following expressions:

$$\mathbf{E}(\mathbf{r}) = \mathbf{E}_j^{\text{ext}} - \frac{1}{\epsilon_j}\int_{S_j} d\mathbf{s}\nabla G_j(\mathbf{r}-\mathbf{s}) \times \mathbf{m}_j(\mathbf{s}) \tag{1}$$

and

$$\mathbf{H}(\mathbf{r}) = \mathbf{H}_j^{\text{ext}} + \mathrm{i}k\int_{S_j} d\mathbf{s}[1 + \frac{1}{k^2\epsilon_j\mu_j}\nabla\nabla]G_j(\mathbf{r}-\mathbf{s})\mathbf{m}_j(\mathbf{s}),$$

where $\mathbf{m}_j$ are magnetic currents parallel to the boundary of region j.

Following Bethe [7], we will use magnetic charges and currents only in the boundary around the hole to solve Maxwell's equations exactly in the presence of a perfect-metal film. He obtained the transmission cross section of a small hole in infinitesimally-thin films by considering a distribution of magnetic charges and currents in the hole, making use of the fact that the induced electric field [i.e., the integral in Eq. (1)] is perpendicular

#1768 - $15.00 US
Received October 28, 2002; Revised December 03, 2002

to the film at its surface. He worked out an analytical expression in the long wavelength limit (see below), in which case the magnetic sources can be regarded as a magnetic dipole. Our case is slightly more complicated, since we want to solve the problem for an arbitrary size of the hole and for films of finite thickness. However, Bethe's ideas can be still applied by considering the construction sketched in Fig. 1: the magnetic boundary sources in regions I and III (right on the upper and lower sides of the hole, respectively), do not contribute to the parallel electric field on their respective side of the film surface. The boundary sources in the inner region of the hole are then used to match the electromagnetic field in that region to the field outside it.

Now, the external field is taken to be a plane wave reflected on an infinite metallic film, so that the parallel components of $\mathbf{E}_j^{\text{ext}}$ vanish at the film surfaces. Therefore, the boundary conditions at the film surfaces are just satisfied because the parallel components of both external and induced fields vanish altogether by construction. The actual solution of the boundary sources is obtained by discretizing the boundary of the hole, which will be described by a set of representative points. Two values of the magnetic current are defined at each of these points in the upper and lower parts of the hole: one for the vacuum side and a different one for the inner side. Also, the parallel components of the electric and magnetic fields are set to be continuous at each discretization point [12], so that the number of equations (2 two-component vector equations per point) equals the number of variables (2 two-component parallel currents). On the vertical boundaries of the hole, there is only one condition per discretization point (i.e., the vanishing of the parallel electric field), but no current has to be defined on the metal side of the boundary, so that the total number of variables and equations remains equal to each other.

The symmetry of the geometry under consideration allows us to use cylindrical coordinates to solve the problem, and in particular for normal incidence only the $m = \pm 1$ components are relevant, which lowers the dimensionality of the numerical method to 1.

A typical solution of this problem is presented in Fig. 2, where the transmission cross section is represented as a function of the radius of the hole for a film thickness t equal to 0.1 times the radius a and for light incident normally to the film. The cross section is defined as the area by which one has to multiply the incoming photon flux per unit area to obtain the transmitted photon flux. The cross section has been normalized to the area of the hole in the plot. Obviously, this ratio has to go to 1 in the small wavelength limit, and this can be already observed for holes as small as the wavelength in diameter. Notice that the transmission presents a maximum in the subwavelength regime for $a = 0.27\lambda$.

In the related context of slits in metallic films, the transmission of light polarized perpendicularly to the aperture can reach cross sections that are several orders of magnitude larger than the aperture area [5, 6]. This is the result of Fabry-Pérot resonances in the narrow channel formed by the slit and involving evanescent modes of the waveguide [13, 14, 15]. However, such resonances do not occur when the electric-field polarization is along the slit [5, 6], in which case the resulting transmission is very small. Similarly, one can attribute the maximum in transmission observed in Fig. 2 to such a type of resonance, although in the case of circular holes the incident electric field is not perpendicular to the aperture edge in all of its contour, and this, together with the finite size of the aperture, causes an attenuation of the strength of the mentioned resonance as compared to the case of the slit.

In our case, the relevant modes of the circular waveguide can be propagating. Indeed, whereas the condition required by a square waveguide drilled in a perfect metal material to sustain propagating modes is that its side is not smaller than half the wavelength, the

#1768 - $15.00 US Received October 28, 2002; Revised December 03, 2002

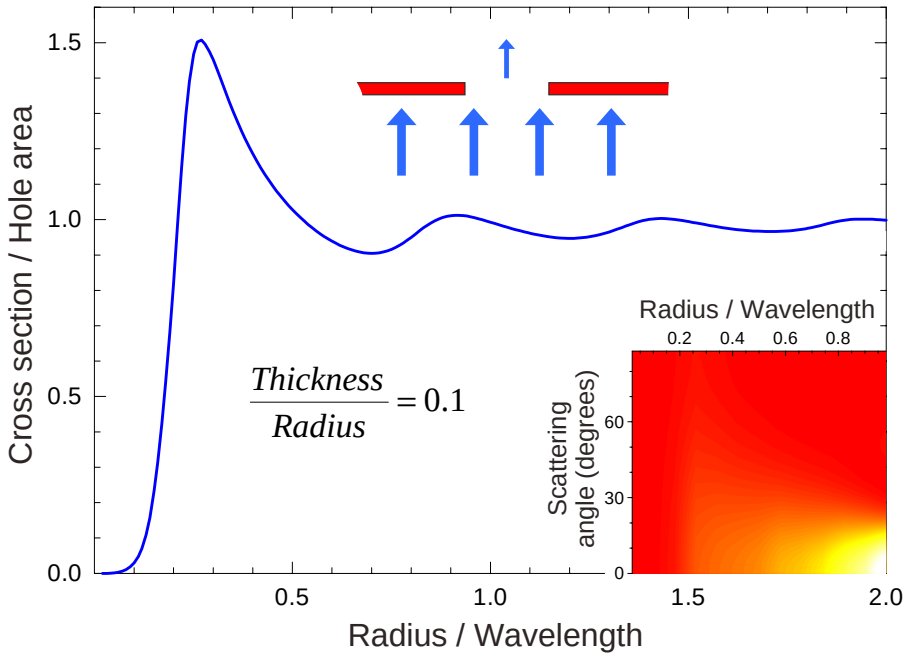

Fig. 2. Transmission cross section of a cylindrical hole in a perfect-metal slab as a function of the hole radius. The slab thickness is 0.1 times the radius. The cross section is normalized to the area of the hole, and the radius is normalized to the wavelength. The incidence of the light is perpendicular to the slab. The contour-plot inset shows the polar angle distribution of transmitted light as a function of hole radius (brighter regions stand for higher transmission intensity).

#1768 - $15.00 US
Received October 28, 2002; Revised December 03, 2002

case of circular waveguides is governed by zeros of Bessel functions and its derivative, which under normal incidence (i.e., for fields belonging to the $m = 1$ symmetry) imply that ka must be above the first zero of J_1', that is, $a > 0.3\lambda$. This limiting value is close to where the resonance is observed in the transmission curve of Fig. 2.

The inset of Fig. 2 shows that the angular distribution of the transmitted light is very broad for small radius, whereas it is highly directly along the propagation direction of the incoming beam as the hole radius increases. In connection to this, the presence of additional structure on the exit surface of the film has been recently shown to greatly modify this angular dependence of the transmission [3].

Figure 3(a) shows the results obtained for different ratios of the film thickness to the radius of the hole, t/a. As the relative thickness increases, the transmission diminishes considerably in the subwavelength region. In Fig. 3(b) these calculations are represented in logarithmic scale, showing the expected $\propto (a/\lambda)^4$ dependence of the transmission in the small-hole limit [7]. The actual value of the transmission for a given radius decreases nearly exponentially with film thickness in the long wavelength limit, and this permits one to speculate that the transmission is actually mediated by evanescent modes that propagate along the hole. However, the maximum of transmission [Fig. 3(a)] shifts towards larger values of the radius as the thickness increases and its actual value does not decrease exponentially, but rather seems to approach a limiting value. This behavior could be due to the contribution coming from transmission mediated by propagating modes of the circular waveguide, as discussed above.

The results of Fig. 3 have been compared with the analytical formula

$$\frac{\sigma}{\pi a^2} = \frac{64}{27\pi^2}(ka)^4[1 + \frac{22}{25}(ka)^2 + \frac{7312}{18375}(ka)^4 + \ldots], \quad (2)$$

which applies to infinitesimally-thin films ($ka = 2\pi/\lambda \ll 1$). The first term in this expression was first derived by Bethe [7] and subsequent terms were calculated later on by Bouwkamp [8]. Equation (2) is in good agreement with the extrapolated behavior of the calculations presented in Fig. 3(b) to zero thickness within the large wavelength limit. However, Fig. 3(b) also indicates that Eq. (2) is rather inaccurate for a radius as small as 0.2 times the wavelength, and while the Bouwkamp correction terms describe the change in slope actually better than Bethe's first term in Eq. (2) within the $0.07 < a/\lambda < 0.15$ range, the former breaks down earlier as a/λ increases.

Dielectrics are to light what metals are to electrons in the sense that Helmholz equation for light in a material of dielectric function larger than one can be rewritten as Schrödinger equation with a negative potential. So, one could expect that light would be attracted to the hole if one filled it with a high-index dielectric material, and this would in turn result in improved transmission. This is actually the case, as shown in Fig. 4 for a hole filled with Si ($\epsilon = 11.9$). The transmission resonance in the subwavelength region reaches a cross section that is nearly three times the area of the hole, and a factor of two larger than that of the undressed hole (see Fig. 2). Besides, the resonance is considerably narrower when the hole is filled with Si. The transmittance of a homogeneous Si film of the same thickness is also given in Fig. 4 for comparison (broken curve showing a smooth dependence on wavelength, as the resonances in the solid curve are connected with the presence of the hole, which is missing in the homogeneous Si film considered in the broken curve). The normalized cross section of the hole converges to the transmittance through a homogeneous Si film in the large radius limit. In addition to the main resonance near $a = 0.18\lambda$, a series of resonances is observed in this case for larger radius, which originate in the reduction of the wavelength by a factor of nearly 3.5 in Si as compared to the wavelength in vacuum, so that more propagating modes are switched on within the range of radius under consideration. The narrowing of the resonance could also

#1768 - $15.00 US Received October 28, 2002; Revised December 03, 2002

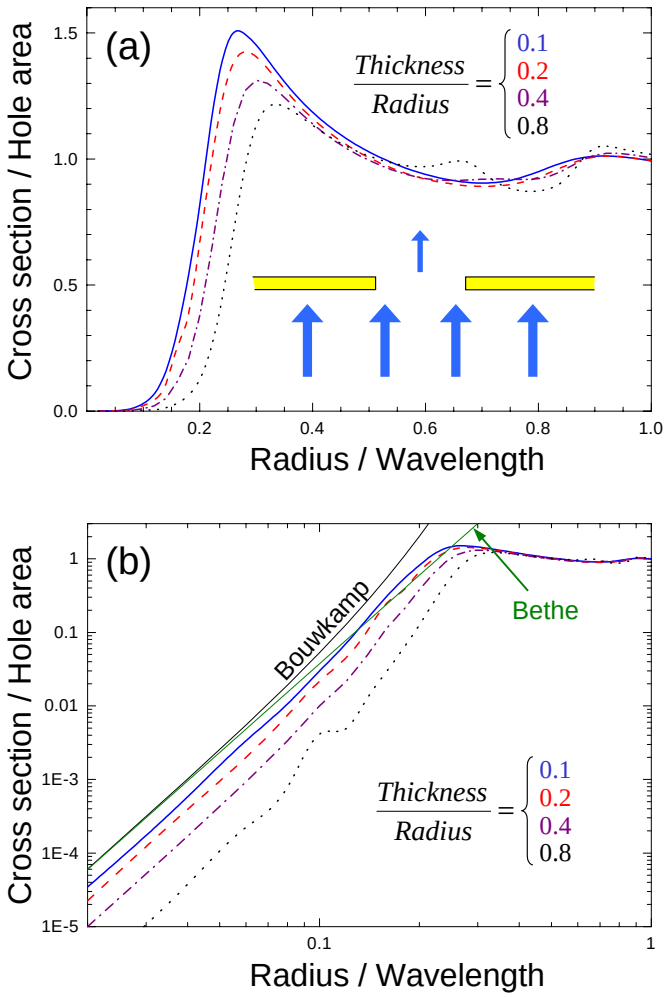

Fig. 3. **(a)** Transmission cross section of a cylindrical hole drilled in a perfect-metal film as a function of the hole radius for different ratios of the slab thickness to the radius (see labels). The light is coming perpendicular to the film. **(b)** Same as (a) in log − log scale and compared with the asymptotic formulas of Bethe (Ref. [7]) and Bouwkamp (Ref. [8]), which are valid for vanishing thickness [see Eq. (2)].

#1768 - $15.00 US
Received October 28, 2002; Revised December 03, 2002

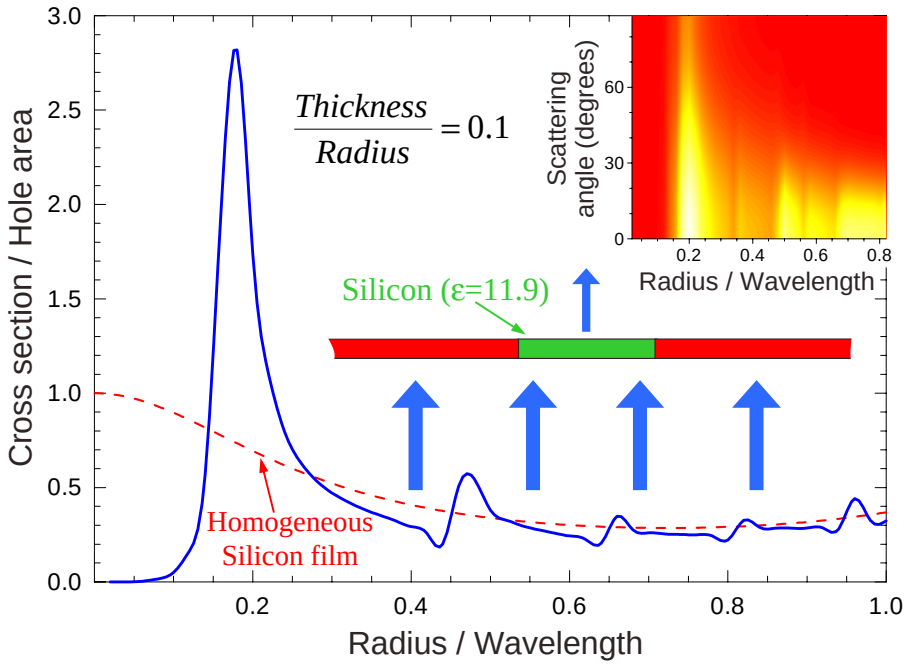

Fig. 4. Transmission cross section of a cylindrical hole drilled in a perfect-metal thin film and filled with Si (solid curve) as a function of hole radius. The broken curve represents the transmittance of a homogeneous Si film of the same thickness. The dependence of the transmitted intensity on the polar angle upon exit is shown in the inset (brighter regions stand for higher transmission intensity).

#1768 - $15.00 US
Received October 28, 2002; Revised December 03, 2002

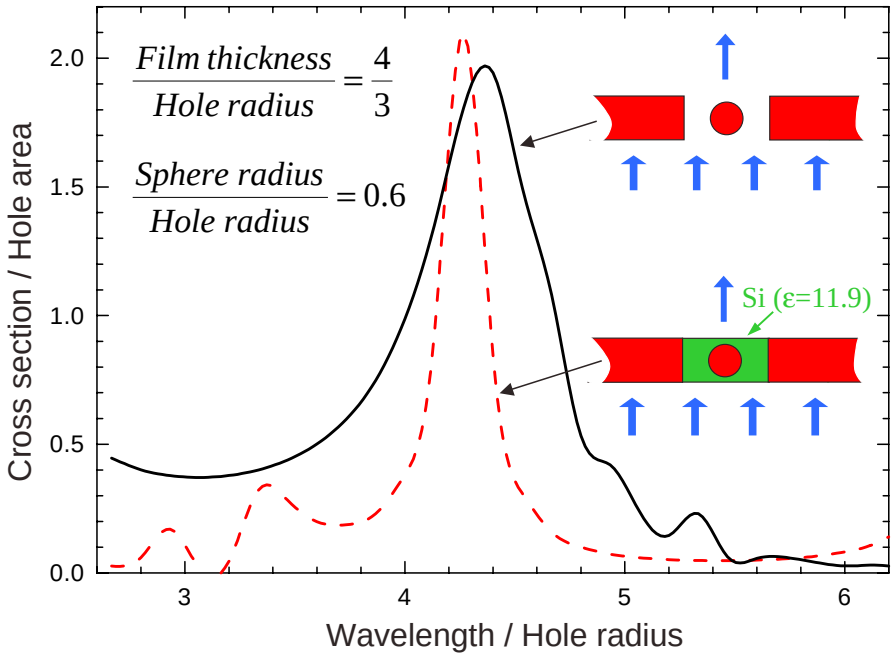

Fig. 5. Transmission cross section of a cylindrical hole drilled in a perfect-metal thin film and containing a perfect-metal sphere in its center (solid curve). The light is coming perpendicular to the film. The broken curve corresponds to the transmission of the same geometry but with the hole filled with Si (see insets).

originate from this contraction of the wavelength. This argument would lead also to an effective film thickness that is larger by the same factor, but the height of the peak is larger than in the case of the naked hole of the same thickness considered above, so that the coupling mechanism of the external light to propagating modes of the circular waveguide is certainly complex.

Finally, the effect of introducing additional structure inside the hole has been illustrated in Fig. 5. A perfect-metal sphere has been placed inside the hole and the resulting normalized cross section is slightly larger than in the case of the undressed hole (Fig. 2). If the hole is now filled with Si (dashed curve in Fig. 5), the width of the resonance is significantly reduced, as it occurred in the hole without the sphere. The modification of the resonance introduced by the sphere can be significant, as one can see in the vanishing of the transmittance near $\lambda = 3.2a$ in the broken curve.

In summary, the transmission of light through a single cylindrical hole in a perfect-metal film has been studied by solving Maxwell's equations using a modified version of the boundary element method. The transmission has been shown to exhibit a resonance in the subwavelength region that is attributed to the resonant coupling with propagating modes of the cylindrical cavity defined by the hole. The case of films of finite thickness has been addressed and their long-wavelength limit behavior has been compared to the

#1768 - $15.00 US
Received October 28, 2002; Revised December 03, 2002

analytical formulas of Bethe [7] and Bouwkamp [8], which have been shown to be valid only for a radius smaller than 0.2 times the wavelength. The presence of additional structures inside the hole has been shown to modify the transmission modes and their corresponding transmission resonances. The effect of filling the hole with a high-index material has also been shown to lead to improved transmission cross sections and narrow transmission resonances, suggesting a way to actually construct light funnels in the subwavelength domain.

The author gratefully acknowledges help and support from the Basque Departamento de Educación, Universidades e Investigación, the University of the Basque Country UPV/EHU (contract No. 00206.215-13639/2001), and the Spanish Ministerio de Ciencia y Tecnología (contract No. MAT2001-0946).

#1768 - $15.00 US Received October 28, 2002; Revised December 03, 2002